Colloid Polym Sci 274:854–859 (1996)

ORIGINAL CONTRIBUTION

M.A. Morini
R.M. Minardi
P.C. Schulz
J.L. Rodriguez

The effect of NaOH on dodecyltrimethylammonium hydroxide aggregation in aqueous solutions

Received: 18 September 1995
Accepted: 23 January 1996

M.A. Morini · R.M. Minardi
Prof. P.C. Schulz (✉) · J.L. Rodriguez
Universidad Nacional del Sur
Department of Chemistry and
Chemical Engineering
Universidad Nacional del Sur
8000 Bahia Blanca, Argentina

Abstract The aggregation of dodecyltrimethylammonium hydroxide (DTAOH) in aqueous NaOH solutions was studied as a function of NaOH concentration. As in NaOH-free DTAOH aqueous solutions, the surfactant underwent a stepwise aggregation mechanism. Changes in the structure of aggregates produced an increase of the concentration at which premicellar aggregates could solubilize hydrophobic dyes and also in the concentration at which hydroxide ions join the aggregates.

Key words Hydroxide surfactants – critical micelle concentration – aggregation – cationic surfactants – counterion effect

Introduction

Knowledge of the properties of hydroxide surfactants is of great interest in the theoretical interpretation of micellar catalysis [1, 2]. There is some counterintuitive information about the behavior of hydroxide surfactants [3], and the properties of their micelles differ strongly from that of other surfactants with different counterions [4]. In a previous paper [5], we found that dodecyltrimethylammonium hydroxide (DTAOH)-water solutions undergo a stepwise aggregation process. Here, we studied the aggregation behavior of DTAOH with aggregated NaOH. As in the previous paper, in this work the DTAOH aggregation was studied by methods that measure properties of the system as a whole (conductivity), properties mainly depending on the single-dissolved species activity (surface tension, DTA^+ ion-selective electrode, pH electrode) and on the micelles (dye solubilization, density, changes in Rhodamine 6G fluorescence and colour).

Experimental

The preparation on dodecyltrimethylammonium hydroxide (DTAOH) was reported elsewhere [5]. A concentrated LTAOH solution was used to prepare dilutions with a fixed NaOH concentration in double-distilled, CO_2-free water. Much care was taken to avoid contamination with atmospheric CO_2 in this work. Details may be found in ref. [5].

The study of the aggregation steps on the DTAOH solutions was performed in the same way as in the previous paper [5], and only the modifications are reported here. Only Sudan Black B was employed in the dye solubilization measurements, because Sudan Red III is soluble in NaOH aqueous solutions. All runs were performed at $25.0 \pm 0.1\,^{\circ}C$, by water circulation from a thermostat.

When straight lines were obtained, they were treated using the least squares method. Averages were obtained with the minimum variance linear unbiased estimation method [6]. A confidence level of 0.90 and Student's **t** distribution function was employed in all error estimations.

Results

The plots of the density, dye solubilization, surface tension and glass electrode measurements were similar to that in NaOH-free aqueous DTAOH solutions [5].

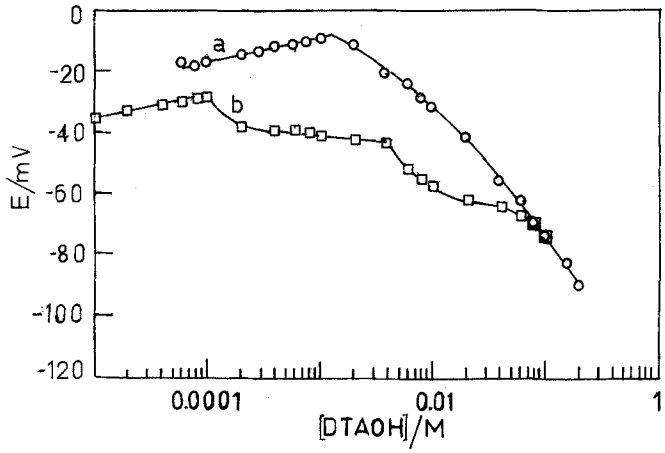

Fig. 1 DTA^+ ion-selective electrode potential vs. DTAOH concentration. DTAOH aqueous solutions with **A)** 10^{-4} mol·dm^{-3} NaOH, **B)** 5×10^{-2} mol·dm^{-3} NaOH

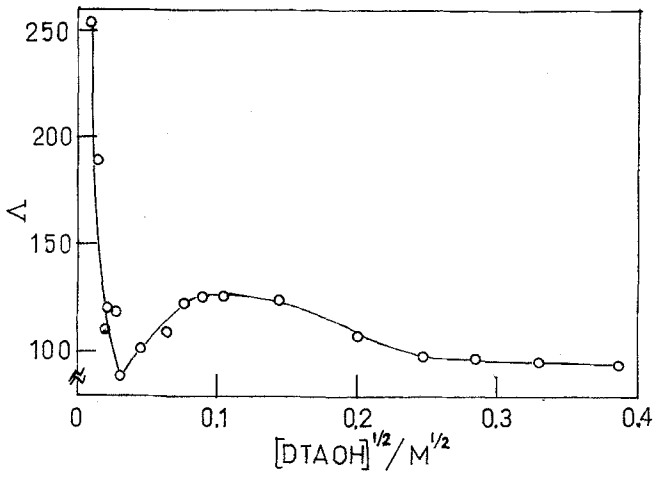

Fig. 3 Equivalent conductivity of aqueous DTAOH + 0.01 mol·dm^{-3} NaOH

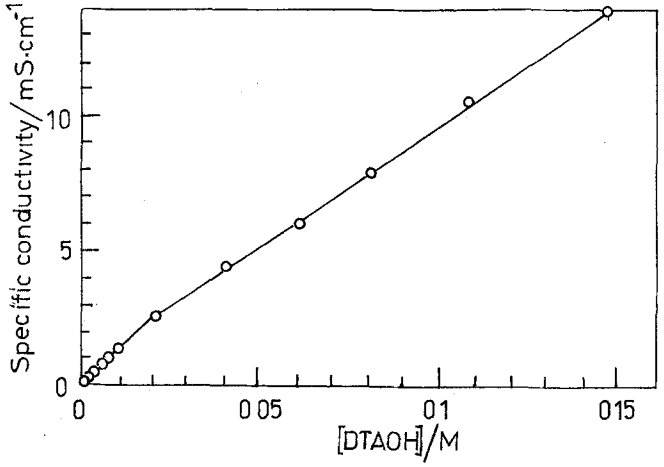

Fig. 2 Specific conductivity of aqueous DTAOH + 0.01 mol·dm^{-3} NaOH

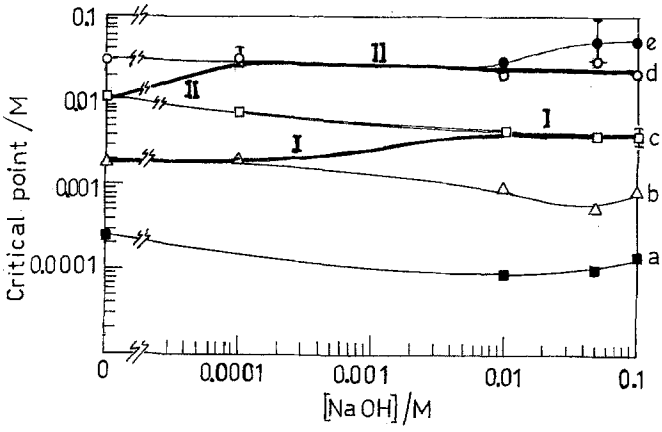

Fig. 4 Average critical points of DTAOH aqueous solutions vs. concentration of added NaOH

Here, we report only the figures which show some substantial differences with that shown in the previous paper [5].

Figure 1 shows DTA^+ ion-selective electrode results in DTAOH aqueous solutions with a) 0.0001 mol·dm^{-3} NaOH and b) 0.05 mol·dm^{-3} NaOH.

Figures 2 and 3 show the specific and equivalent conductivity of aqueous DTAOH + 0.01 mol·dm^{-3} NaOH.

The determined critical points are reported in Table 1, and average values were plotted in Fig. 4.

Discussion

The interpretation of the density, dye solubilization, surface tension and glass electrode measurements was similar to that in NaOH-free aqueous DTAOH solutions [5]. We shall discuss in some detail the data which showed differences with that in NaOH-free aqueous DTAOH solutions.

The DTA^+ ion-selective electrode, which is sensitive to single DTA^+ ions activity, indicates that the aggregation of these ions starts at point "a". For 0 and 0.0001 mol·dm^{-3} of added NaOH the curves are smooth after the break, but for larger NaOH concentrations several breaks may be seen (Fig. 1). These breaks occur at concentrations in which other methods also show critical points.

The conductivity and surface tension data obtained are similar to those of Zimmels et al. [7, 8]. According to these authors, this type of behavior corresponds to a stepwise aggregation.

Many authors have reported on systems which have multiple critical concentrations (see ref. [8] and refs.

Colloid & Polymer Science, Vol. 274, No. 9 (1996)

Table 1 Critical aggregation points determined with different methods on aqueous solutions of DTAOH + NaOH ($mol \cdot dm^{-3}$)

[NaOH] = 0 Method	Point a	Point b	Point c	Point d
Literature data				0.0305 ± 0.0030 [21] 0.0295 ± 0.0020 [21]
		7.7×10^{-4} [21, 27]		
				0.033 [3]
	$2.506 \times 10^{-4} \pm 0.099 \times 10^{-4}$	$1.896 \times 10^{-3} \pm 0.071 \times 10^{-3}$	$1.108 \times 10^{-2} \pm 0.010 \times 10^{-2}$	0.0302 ± 0.0028 [5]
Average values	$2.506 \times 10^{-4} \pm 0.099 \times 10^{-4}$	$1.896 \times 10^{-3} \pm 0.071 \times 10^{-3}$	$1.108 \times 10^{-2} \pm 0.010 \times 10^{-2}$	0.03199 ± 0.00082

$[NaOH] = 10^{-4}$ M Method	Point a	Point b	Point c	Point d
Surface tension		$1.5 \times 10^{-3} \pm 1.4 \times 10^{-3}$	$8.9 \times 10^{-3} \pm 4.2 \times 10^{-3}$	0.03
Conductivity		$1.9 \times 10^{-3} \pm 0.1 \times 10^{-3}$	$8.9 \times 10^{-3} \pm 4.2 \times 10^{-3}$	0.04
Glass electrode				0.026
DTA^+-ion selective electrode		$2.4 \times 10^{-3} \pm 0.7 \times 10^{-3}$		
Solubility (Sudan Black B)		$2.4 \times 10^{-3} \pm 1.4 \times 10^{-3}$		
Density			$6.4 \times 10^{-3} \pm 2.1 \times 10^{-3}$	
Average values		$1.90 \times 10^{-3} \pm 0.09 \times 10^{-3}$	$6.943 \times 10^{-3} \pm 0.004 \times 10^{-3}$	0.039 ± 0.007

$[NaOH] = 10^{-2}$ M Method	Point a	Point b	Point c	Point d	Point e
Surface tension		$8.2 \times 10^{-4} \pm 1.4 \times 10^{-4}$		0.02206 ± 0.00033	
Conductivity	$2.0 \times 10^{-4} \pm 0.1 \times 10^{-4}$	$9.3 \times 10^{-4} \pm 0.1 \times 10^{-4}$		0.0171 ± 0.0014	
Glass electrode				0.0104 ± 0.0093	0.03 ± 0.44
DTA^+-ion selective electrode	$2.1 \times 10^{-5} \pm 0.1 \times 10^{-5}$		$4.5 \times 10^{-3} \pm 0.1 \times 10^{-3}$		0.030 ± 0.001
Solubility (Sudan Black B)			$1.5 \times 10^{-3} \pm 1.0 \times 10^{-3}$		
Rhodamine 6G					0.05 ± 0.01
Density					0.039 ± 0.015
Average values	$9.1 \times 10^{-5} \pm 0.1 \times 10^{-4}$	$9.30 \times 10^{-4} \pm 0.01 \times 10^{-4}$	$4.23 \times 10^{-3} \pm 0.07 \times 10^{-3}$	0.0218 ± 0.0003	0.030 ± 0.001

$[NaOH] = 5 \times 10^{-2}$ M Method	Point a	Point b	Point c	Point d	Point e
Surface tension		$1.3 \times 10^{-3} \pm 2.3 \times 10^{-3}$	$5.02 \times 10^{-3} \pm 0.01 \times 10^{-3}$		0.05 ± 0.12
Conductivity	$1.0 \times 10^{-4} \pm 0.1 \times 10^{-4}$	$5.5 \times 10^{-4} \pm 0.2 \times 10^{-4}$	$2.5 \times 10^{-3} \pm 1.0 \times 10^{-3}$	0.0322 ± 0.0007	
Glass electrode				0.033 ± 0.015	
DTA^+-ion selective electrode	$1.0 \times 10^{-4} \pm 0.1 \times 10^{-4}$		$4.0 \times 10^{-3} \pm 0.1 \times 10^{-3}$	0.030 ± 0.001	
Solubility			4.6×10^{-3}		

Table 1 Continued

Method	Point a	Point b	Point c	Pointd	Point e
(Sudan Black B)			$\pm 0.9 \times 10^{-3}$		
Rhodamine 6G				0.03	
				± 0.01	
Density				0.030	
				± 0.002	
Average values	1.01×10^{-4}	5.5×10^{-4}	4.0×10^{-3}	0.0313	0.05
	$\pm 0.07 \times 10^{-4}$	$\pm 0.7 \times 10^{-4}$	$\pm 0.1 \times 10^{-3}$	± 0.0006	± 0.12
$[NaOH] = 10^{-1}$ M					
Method	Point a	Point b	Point c	Point d	Point e
Surface				0.008	0.036
tension				± 0.007	± 0.018
Conductivity	2.0×10^{-4}	8.9×10^{-4}		0.0226	
	$\pm 0.1 \times 10^{-4}$	$\pm 0.1 \times 10^{-4}$		± 0.0012	
Glass				0.028	
electrode				± 0.014	
DTA^+-ion	1.0×10^{-4}		4.0×10^{-3}		0.050
selective electrode	$\pm 0.1 \times 10^{-4}$		$\pm 0.1 \times 10^{-3}$		± 0.001
Solubility			4.1×10^{-3}		
(Sudan Black B)			$\pm 0.1 \times 10^{-3}$		
Rhodamine 6G				0.03	
				± 0.01	
Density					0.040
					± 0.035
Average values	1.49×10^{-4}	8.9×10^{-4}	4.1×10^{-3}	0.0223	0.050
	$\pm 0.07 \times 10^{-4}$	$\pm 0.1 \times 10^{-4}$	$\pm 0.9 \times 10^{-3}$	± 0.0012	± 0.001

therein, [9]). In particular, there is conclusive evidence about the formation of premicellar aggregates as dimers [7, 10, 11] and larger aggregates [13, 14].

Small, fully ionized aggregates formed at point "a"; these cannot solubilize hydrophobic molecules, like the aggregates proposed by Bunton et al. [3].

At this point the equivalent conductivity rises because the fully ionized aggregates are better conductors than the separate monomers. Points "a" shifted to lower concentrations when the NaOH concentration was raised.

At point "b" another transformation occurred. With 0 and 0.0001 $mol \cdot dm^{-3}$ NaOH the aggregates can solubilize Sudan Black B molecules, which are uncharged in alkaline solutions. However, at higher NaOH concentrations, the dye solubilization occurs at point "c". Point "b" shifted to lower concentrations when the NaOH concentration was raised. Point "b" may be the minimum multimerization concentration (MMC) defined by Funasaki [15] as the concentration at which aggregates with more than three monomers form.

Bunton et al. [16] found that hexadecyltrimethylammonium hydroxide (CTAOH) and fluoride (CTAF) systems show a large range of aggregate sizes. There are small aggregates at low concentration, but their size increases with surfactant concentration until they become true micelles.

Point "c" also shifted to lower concentrations when the NaOH concentration was raised. If no NaOH is added, at this point the aggregation of counterions to the aggregates to form common micelles will start (i.e., large aggregates with counterions which are part of the kinetic entity), but when NaOH is added, this aggregation of counterions shifted to point "d". Since at this point the micelles are small ($n = 20$ [4]) and highly charged ($\alpha = 0.74 - 0.63$ [2, 4], 0.80 [5]), their contribution to the total conductivity of the system must be high. The conductivity of the OH^- counterions (which are predominantly non-micellized) is very high, so the real CMC is almost undetectable by conductivity measurements.

In the absence of NaOH, point "d" corresponds to a change in micelle structure [5], and this may be the interpretation of point "e", at NaOH concentrations higher than 0.01 $mol \cdot dm^{-3}$, following the model proposed by Zimmels and Lin [9b, 17]. The specific conductivity showed a break, which may indicate the presence of almost uncharged micelles, as in NaOH-free DTAOH solutions [5]. Rhodamine 6G, which has a positive charge, detects micelles at this point. This is probably due to its

adsorption on the micelle surface when the (positive) surface potential is small enough. Density changes also occur at this point.

As was pointed out in the literature, the structure of micelles changes with the counterion concentration [18]. This change occurs in a wide range of concentrations with hydrophilic ions such as OH^- or F^- [19,20], and in a narrower one with hydrophobic ions as Br^- [16]. Paredes et al. determined the heat of micellization of CTAC, CTAF and CTAB in water, this monotonically increases with surfactant concentration, whereas that of CTAOH has a maximum (Figs. 2–5 of the paper of Paredes et al. [21]). This may indicate postmicellar changes in structure with increasing concentration.

Many other systems (soaps, bile salts, bolaform amphiphiles) show evidence of postmicellar critical points [9a–9c, 22].

In Fig. 4, curves "a", "b", "c", "d" and "e" represent steps in the stepwise aggregation process of DTAOH. Curve "a" is the concentration at which the aggregation starts. Curve I represents the concentration at which the fully ionized aggregates are able to solubilize hydrophobic molecules. Curve II is the concentration at which the counterions join the aggregates, forming "classical" micelles which includes counterions in the Stern layer.

Curves I and II rise with NaOH concentration. In many ways, the behavior of hydroxide surfactants is counterintuitive [3]. The CMC determined by Paredes et al. for tetradecyltrimethylammonium hydroxide (TTAOH) and CTAOH decreased with increasing counterion concentration [21]. They determined the CMC of these surfactants by surface tension measurements, which corresponds to our points "b". As can be seen in Fig. 4, point "b" also decreased with increasing NaOH concentration, but may not be interpreted as the CMC of the surfactant.

There are different CMC definitions [23], and this is a source of difficulties when systems with stepwise aggregation are studied. In addition, the value of the CMC for a surfactant system depends on the experimental technique, its analysis and the concentration range [15]. Curve II is probably the phenomenon closest to the "classical" CMC in the DTAOH-water system.

Some thermodynamic properties of RTAOH solutions in the literature may be related to the unusual behavior of curves I and II. The specificity of the binding of counterions to micelles is related to the enthalpic contribution to the total free energy for the transference of a given counterion from water to the micellar interface. The dehydration and location of the counterion in the Stern layer play an important role in this contribution [21].

The heat of micellization of alkyltrimethylammonium salts as a function of the concentration of added counterions monotonically increases for CTAC, $CTANO_3$ and CTAB, whereas that of CTAF, CTAOH and TTAOH decreases with the increase of F^- or OH^- concentration, and passes through a slight minimum (see Fig. 6 of Paredes et al. [21]).

In the case of CTAOH, the entropy of micellization has a maximum when the NaOH concentration increases (see Table I of Paredes et al. [21]). This entropy can be separated into two contributions: one constant contribution independent of the counterion concentration due to the hydrophobic effect produced by the transfer of the hydrocarbon chain from water to the micelle and other due to the binding of the counterion to the micellar charged surface [21]. Thus, the variation of the micellization entropy is probably due to a different mode of counterion binding. The maximum is at 0.005 M of added NaOH. The decrease in ΔS_m at larger NaOH concentrations may be due to a decrease in the counterion binding.

In the above results, it may be seen that on increasing the NaOH concentration, the thermodynamic properties of RTAOH micelles behave differently from that of RTAX with X^- addition. These thermodynamic properties are closely related to aggregation, and similar unusual behavior was observed in our results.

The interaction of DTAOH aggregates with OH^- ions is qualitatively different from that of RTAX with X^- ions. The hydroxide radical must be located, on average, about 0.4 nm further out from the charged surfactant head group than for the bromides [3]. This is a consequence of the extreme hydrophilic nature of the hydroxyl anion in water. The resulting increased Coulombic repulsion between the surfactant head groups gives increased head-group area, increased surface curvature, and decreased aggregation number. The concentration of HO^- ions in the RTAOH micelle Stern layer is well below that of Br^- in the same region in RTAB micelles [4].

As a consequence of this difference, the properties of RTAOH micelles are unusual. The micelle aggregation number for tetradecyltrimethylammonium hydroxide changes only from 45 to 70 over the concentration range 0–1 $mol \cdot dm^{-3}$ NaOH. The effective volume fraction of micelles in this system was almost constant on addition of NaOH. Large changes in micelle size and charge are not observed when NaOH is added to DTAOH aqueous solutions, unlike the DTAB solutions behavior [3].

Curve II may reflect these unusual interactions between micelles and hydroxide ions. The phenomena may represent changes in micellar structure as well as ionic distribution [24].

The behavior of curve I may be due to changes in the structure of aggregates with NaOH addition. RTAOH micelles are small and spherical. This suggests that the alkyl chains in the micelle are ordered in different manner

in RTAOH than in RTAX micelles [4]. In agreement with this view, the microviscosity of RTAOH micelles was found to be two- to threefold larger than that of RTAB micelles [25]. Hydrodynamic results on hydroxide surfactants suggest that there is rapid exchange between species in solution [3]. Whatever small hydroxide surfactant aggregates are formed must be extremely labile [3]. Added OH may interact with DTAOH micelles or other submicroscopic aggregates to change their structure [16, 26]. Thus, changes in structure instead of changes in size, may be responsible for the changes in the solubilization capacity of aggregates.

Changes in the structure of aggregates may cause an increase of the concentrations at which premicellar aggregates can solubilize hydrophobic dyes and the concentration in which hydroxide ions joint the aggregates.

In view of the results of this work and the preceding paper [5] about the complex multiple-step aggregation process of DTAOH aqueous solutions, the question arises of whether the pseudophase separation model of micellization is applicable or not to this and other related systems. This assertion has been made by Bunton et al. [16, 24] and is of great importance in the interpretation of micellar catalysis results.

Work is in progress to elucidate the structure of micelles and premicellar aggregates.

Conclusions

The aggregation of Dodecyltrimethylammonium hydroxide in aqueous NaOH solutions follows a stepwise mechanism.

Acknowledgments Two of us (M.A.M and R.M.M.) hold a fellowship from the Consejo Nacional de Investigaciones Cientificas y Técnicas (CONICET) de la República Argentina. This work was supported by a grant of the Universidad Nacional del Sur.

References

1. de Graça Nascimento M, Miranda SAF, Nome F (1986) J Phys Chem 90:3366
2. Ortega F, Rodenas E (1987) J Phys Chem 91:837
3. Ninham BW, Evans DF, Wei GJ (1983) J Phys Chem 87:5020
4. Lianos P, Zana R (1983) J Phys Chem 87:1289
5. Schulz PC, Morini MA, Minardi RM, Puig JE, Colloid Polym Sci (in press)
6. Mandel J (1964) Statistical Analysis of Experimental Data Interscience Pub Co New York
7. Zimmels Y, Lin IJ (1974) Colloid Polymer Sci 252:594
8. Zimmels Y, Lon IJ, Friend JP (1975) Colloid Polym Sci 253:404
9. a) Sköld RO, Tunius MAR (1992) J Colloid Interface Sci 152 (1):183; b) Danielsson I (1956) Acta Acad Abo Ser B XX (15):165; c) Meguro K, Ikeda K, Otsuji A, Taya M, Yasuda M, Esumi K (1987) J Colloid Interface Sci 118:372; d) Elworthy PH (1959) J Pharm Pharmacol 11:557; e) Bhalekar AA, Engberts JBFN (1993) Colloid Polym Sci 271:1068
10. Kale KM, Kussler EL, Evans DF (1982) J Soln Chem 11(8):581
11. Mukerjee P (1965) J Phys Chem 69:2821
12. Shedlowsky L, Jacob CW, Epstein MB (1963) J Phys Chem 67:2075
13. Stenius P, Zilliacus CH (1971) Acta Chem Scand 25(6):2232
14. Stenius P (1969) Chim Phys Appl Prat Ag Surface C R Congr Inter Deterg 5th Sept 1968 09–13:1023
15. Funasaki N (1993) Advan Colloid Interface Sci 43:87
16. Bunton C, Gan L, Moffat J, Romsted L, Savelli G (1981) J Phys Chem 85:4118
17. Sheppard SE (1942) Rev Mod Phys 14:303
18. Bunton CA, Frankson J, Romsted IS (1980) J Phys Chem 84:2607
19. Gunnarsson G, Johnsson B, Wennerstrom H (1980) J Phys Chem 84:3114
20. Rohde A, Sackmann E (1979) J Colloid Interface Sci 70:494 – (1980) J Phys Chem 84:1598
21. Paredes S, Tribout M, Sepúlveda L (1984) J Phys Chem 88:1871
22. a) Ekwall P (1964) Proc IVth Internat Congress on Surf Activ Subst p 651; b) Ekwall P, Lemström KE, Eikrem H, Holmberg P (1967) Acta Chem Scand 21:1402; c) Ekwall P, Danielsson I, Stenius P (1972) in M T P International Review of Science Surface Chemistry and Colloids Physical Chemistry, London Vol 7 p 97; d) Wolfram E, Boross V (1971) Forschrittsber Kolloid Polymer 55:143; e) Durand RR, Yvette W (1968) C R Acad Sci Paris, Ser C 266 (25):1658; f) Muller N, Pellerin JH, Chen WW (1972) J Phys Chem 76:1, 3012; g) Ödberg L (1972) J Colloid Interface Sci 41:2, 298
23. a) Watterson JG, Elias HG (1971) Kolloid Z u Z Polymere 249:1136; b) Ruckenstein E, Nagarajan R (1975) J Phys Chem 79:2622; c) Tanford C (1974) J Phys Chem 78:2469; d) Phillips JN (1955) Trans Faraday Soc 51:561
24. Bunton CA, Moffat JR (1992) Langmuir 8:2130
25. Zachariasse M (1978) Chem Phys Lett 57:428
26. Bunton CA, Frankson J, Ronsted LS (1980) J Phys Chem 84:2607
27. Abuin EA, Lissi E, Araujo PS, Aleixo RMV, Chaimovich H, Bianchi N, Miola L, Quina FH (1983) J Colloid Interface Sci 96:293